IEEE Access
Multidisciplinary | Rapid Review | Open Access Journal

Received 31 May 2024, accepted 20 June 2024, date of publication 1 July 2024, date of current version 9 July 2024.

Digital Object Identifier 10.1109/ACCESS.2024.3420951

THEORY

Performance Analysis of Equal-Gain Combining Receivers Over Composite Multipath/ Shadowing Fading Channels

SÁVIO VIEIRA LACERDA DA SILVA[1], LENIN PATRICIO JIMÉNEZ[1], FERNANDO DARÍO ALMEIDA GARCÍA[2], (Senior Member, IEEE), SANTOSH KUMAR[3], JOSÉ CÂNDIDO SILVEIRA SANTOS FILHO[1], (Member, IEEE), EDUARDO RODRIGUES DE LIMA[4], AND GUSTAVO FRAIDENRAICH[1], (Member, IEEE)

[1]Department of Communications, School of Electrical and Computer Engineering, State University of Campinas, Campinas, São Paulo 13083-852, Brazil
[2]Harvard John A. Paulson School of Engineering and Applied Sciences, Harvard University, Cambridge, MA 02138, USA
[3]Department of Physics, Shiv Nadar University, Kalavakkam, Tamil Nadu 603110, India
[4]Department of Hardware Design, Instituto de Pesquisa Eldorado, Campinas, São Paulo 13083-898, Brazil

Corresponding author: Sávio Vieira Lacerda Da Silva (savio.vlacerda@gmail.com)

The work of Sávio Vieira Lacerda Da Silva was supported by the Eldorado Research Institute and Coordenação de Aperfeiçoamento de Pessoal de Nível Superior (CAPES). The work of Lenin Patricio Jiménez was supported by Conselho Nacional de Desenvolvimento Científico e Tecnológico (CNPq) under Grant 141108/2023-1. The work of Fernando Darío Almeida García was supported by São Paulo Research Foundation (FAPESP) under Grant 2022/13901-5. The work of Santosh Kumar was supported by Science and Engineering Research Board (SERB), Department of Science and Technology (DST), Government of India, via under Project CRG/2022/001751.

ABSTRACT In this paper, we assess the performance of an equal-gain combining (EGC) diversity receiver operating over composite Fisher-Snedecor fading channels. The Fisher-Snedecor fading model results from the amalgamation of two well-known physical phenomena that greatly degrade the wireless signal: multipath and shadowing. More precisely, the Fisher-Snedecor $\mathcal{F}$ distribution is formed by the ratio of two independent Nakagami-m random variables (RVs)—the Nakagami-m RV in the numerator models multipath fading while the Nakagami-m RV in the denominator characterizes shadowing fading. To evaluate the performance of the considered EGC diversity receiver, we first derive exact expressions for the probability density function (PDF) and the cumulative distribution function (CDF) of the sum of the ratio of independent Nakagami-m RVs. To achieve this goal, we utilize a Laplace- and residue-based approach. Additionally, we employ the moment-matching method and the Beta Prime distribution to effectively approximate the sum of the ratio of independent Nakagami-m RVs. Subsequently, we apply the obtained exact and approximate sums statistics to compute the performance metrics of the EGC receiver subject to Fisher-Snedecor $\mathcal{F}$ fading channels, such as the outage probability (OP) and the average bit-error rate (ABER). We aspire that the findings presented in this work not only enhance the theoretical comprehension of wireless communication systems but also offer valuable insights for optimizing the design and performance of these systems in real-world scenarios.

INDEX TERMS Beta prime distribution, composite fading channels, equal-gain combing receivers, Fisher-Snedecor $\mathcal{F}$ distribution, sum of the ratio of Nakagami-m random variables.

I. INTRODUCTION

Fading comprises the random variations that a wireless signal experiences and is conventionally classified into two types: (i) multipath and (ii) shadowing [1]. Multipath fading occurs due to signal propagation along multiple paths between the transmitter and receiver. Each path follows a different trajectory to the destination, which is determined by the reflections, diffractions, and scattering of the signal along the route [2]. Shadowing fading, on the other hand, models

The associate editor coordinating the review of this manuscript and approving it for publication was Xueqin Jiang.

the signal variations over large distances where significant obstacles like hills or large buildings obstruct the primary signal path between the transmitter and the receiver.

Classical statistical models such as Rayleigh, Rice, Weibull, and Nakagami-m [3] are commonly used to model multipath fading, while the Log-Normal distribution is considered the most accurate model for characterizing shadowing [4].

Both fading types are usually studied separately. However, in a real scenario, the assumption that the propagated signal solely suffer one kind of fading is not always true. In fact, field measurements have demonstrated that urban/suburban propagation scenarios are better described by models which consider both, multipath fading and shadowing [5], [6]. Those models are known in the literature as composite fading models.

Different statistical models have been proposed as alternatives to characterize the composite fading channel, such as the Nakagami-m/lognormal [7], Rayleigh/lognormal [1], Rice/lognormal [8], Fisher-Snedecor $\mathcal{F}$ [9], α-μ/gamma [10], κ-μ/gamma and η-μ/gamma [11]. Typically, such fading models are distinguished by being derived from the ratio of two random variables (RVs), the first RV (numerator) representing the multipath fading and the second RV (denominator) denoting the shadowing fading (please, cf. [12], [13], [14], [15], [16], [17], [18], [19], [20]).

Among these distributions, the Fisher-Snedecor $\mathcal{F}$ distribution has recently been suggested as an alternative for describing both shadowing and multipath fading, showing an excellent fit to real wireless data [9]. The Fisher-Snedecor $\mathcal{F}$ distribution is formed by the ratio of two independent Nakagami-m random variables (RVs)—the Nakagami-m RV in the numerator models multipath fading[1] while the Nakagami-m RV in the denominator characterizes shadowing fading.

Aiming at enhancing system performance, various wireless communication systems make use of spatial diversity techniques, such as equal-gain combining (EGC) and maximal-ration combining (MRC). MRC offers the best performance. However, its practical implementation poses significant challenges, mainly because it requires both a phase compensation stage and knowledge of the instantaneous fading amplitude at each receiver's branch. On the other hand, EGC does not require knowledge of the instantaneous fading amplitude; it only requires a phase compensation stage at each receiver's branch. As a result, its implementation is significantly simpler compared to that of MRC. More importantly, as the number of branches increases, the performance of EGC receivers approaches that of MRC receivers [4].

[1]The Nakagami-m distribution has been proved to efficiently mimic multipath fading in several wireless applications. Additionally, it encompasses the Rayleigh distribution as a special case, commonly employed for non-line-of-sight scenarios, and can closely approximate the Hoyt and Rice distributions [21], [22].

Within the context of small-scale fading (i.e., multipath) and owing to the simpler implementation and relatively good performance of EGC receivers, several works have examined their performance subject to multipath fading channels like Rayleigh [23], [24], [25], Rice [26], [27], [28], Weibull [29], κ-μ [30], and α-μ [31], [32], [33]. Meanwhile, within the context of composite fading (i.e., multipath and shadowing), other works have concentrated effort to assess the performance of MRC diversity receivers over composite fading channels, such as the Fisher-Snedecor [34], [35] and the Generalized Fisher (GF) [36] fading channels. Specifically, in [34], the performance metrics of MRC receivers, such as the outage probability and the average bit error rate, were derived in terms of the Lauricella multivariate hypergeometric function. In [35], the authors utilized the multivariate Fox's H-function to introduce an alternative expression for the OP, effective capacity, and channel capacities. Similarly, in [36], the ergodic and outage capacities expressions were evaluated using the multivariate Fox's H-function. However, despite many efforts, there are no works addressing the performance of EGC diversity receivers over composite fading channels. The scarcity of studies in the technical literature can be attributed to the complex mathematics associated with the sum of composite fading envelopes. This has motivated the analytical development pursued in this work. More precisely, in this work, we analyze, in an exact (using a Laplace- and residue-based approach) and approximate manner, the performance of EGC receivers operating over Fisher-Snedecor $\mathcal{F}$ fading channels. To the best of our knowledge, no studies have been carried out for the investigated scenario.

The main contributions of this paper can be summarized as follows:

- Exact expressions for the PDF and the CDF of the sum of the ratio of independent Nakagami-m RVs. It is worth emphasizing that the obtained sums statistics serve as valuable analytical tools for wireless engineers, as they can be utilized in various other wireless scenarios, such as multiple scattering communications, multihop relaying systems [37], and cascade fading channels [38].
- Closed-form approximations for the PDF and the CDF of the sum of the ratio of Nakagami-m RVs, given in terms of the Beta Prime statistics.
- A performance assessment of EGC diversity receivers subject to Fisher-Snedecor $\mathcal{F}$ fading channels. Specifically, we derived the essential performance metrics, namely, outage probability (OP) and average bit-error rate (ABER). More interesting, asymptotic expressions for both performance metrics are also introduced in this work.

Notations: In the following, $\mathbb{E}[\cdot]$ denotes expectation; $\Pr[\cdot]$, probability; $\mathbb{N}$, the set of natural numbers; $\frac{1}{2}\mathbb{Z}^+$, the set of positive integer and positive half-integer numbers; $\mathbb{R}^+$, the set of positive real numbers; $\mathbb{C}$, the set of complex numbers;

The remaining sections of this paper are organized as follows. In Section II, we introduce the problem formulation. Following that, in Section III, we provide an exploration of the statistical properties of the distribution of the sum of ratios of Nakagami-m random variables. In Section IV, we outline the calculations necessary to derive the expression that characterizes the composite multipath/shadowing model. Then, Section V presents the results and their respective analyses. Finally, in Section VI, we provide concluding remarks.

II. PROBLEM FORMULATION

Let us define $\{X_n\}_{n=1}^{M}$ and $\{Z_n\}_{n=1}^{M}$ as sets of independent and identically distributed (i.i.d.) Nakagami-m RVs with PDFs given by

$$f_{X_n}(x_n) = \frac{2m_1^{m_1}}{\Gamma(m_1)\Omega_1^{m_1}} x_n^{2m_1-1} \exp\left(-\frac{m_1 x_n^2}{\Omega_1}\right) \tag{1}$$

$$f_{Z_n}(z_n) = \frac{2m_2^{m_2}}{\Gamma(m_2)\Omega_2^{m_2}} z_n^{2m_2-1} \exp\left(-\frac{m_2 z_n^2}{\Omega_2}\right), \tag{2}$$

where m_r and Ω_r ($r \in \{1, 2\}$) represent the shape and spread parameters, respectively, and $\Gamma(\cdot)$ denotes the Gamma function [39].

Additionally, let us define Y as the sum of the ratio of the above defined Nakagami-m RVs, i.e.,

$$Y \triangleq \sum_{n=1}^{M} \frac{X_n}{Z_n}. \tag{3}$$

Since X_n and Z_n are independent RVs, we can equivalently define Y as

$$Y \triangleq \sqrt{\frac{\Omega_1}{\Omega_2}} \sum_{n=1}^{M} H_n = \sqrt{\frac{\Omega_1}{\Omega_2}} \sum_{n=1}^{M} \frac{X_n'}{Z_n'}, \tag{4}$$

where H_n is the ratio of two independent and normalized (i.e., unit power) Nakagami-m RVs X_n' and Z_n', each with PDF given respectively by

$$f_{X_n'}(x_n) = \frac{2m_1^{m_1}}{\Gamma(m_1)} x_n^{2m_1-1} \exp\left(-m_1 x_n^2\right) \tag{5}$$

$$f_{Z_n'}(z_n) = \frac{2m_2^{m_2}}{\Gamma(m_2)} z_n^{2m_2-1} \exp\left(-m_2 z_n^2\right). \tag{6}$$

To the best of our knowledge, there are no closed-form solutions for the exact sum statistics (namely PDF and CDF) of Y. So far, the only method to evaluate the sum statistics in (3) (or, equivalently, in (4)) is through the multi-fold Brennan's integral [40]. Of course, this approach is computationally expensive and prone to convergence and stability problems. In the next section, we address this crucial problem by deriving exact and closed-form approximations for the PDF and the CDF of the sum in (3).

III. SUM STATISTICS

In this section, we furnish exact series representations and closed-form approximations for the sum statistics of Y. To do so, we employ a Laplace- and residue-based approach, as well as the moment-matching method.

A. EXACT SUM STATISTICS

Proposition: The PDF of the sum in (3) can be expressed as a piece-wise function as

$$f_Y(y) = \begin{cases} f_{\mathcal{D}_1}(y), & 0 < y \leq \left(\frac{m_2}{m_1}\right)^{\frac{1}{2}} \\ f_{\mathcal{D}_2}(y), & y > \left(\frac{m_2}{m_1}\right)^{\frac{1}{2}}, \end{cases} \tag{7}$$

where $f_{\mathcal{D}_1}(y)$ is defined as

$$f_{\mathcal{D}_1}(y) = \sqrt{\frac{\Omega_2}{\Omega_1}} \left(\frac{2\left(\frac{m_1}{m_2}\right)^{m_1}}{\Gamma(m_1)\Gamma(m_2)}\right)^{M} \times \sum_{i=0}^{\infty} \frac{\delta_i \left(y\sqrt{\frac{\Omega_2}{\Omega_1}}\right)^{-1+2(i+m_1 M)}}{\Gamma(2(i+M\,m_1))}, \tag{8}$$

where δ_i is given by

$$\delta_0 = (\Gamma(m_1+m_2)\Gamma(2m_1))^M \; \delta_i = \frac{1}{i\,\Gamma(m_1+m_2)\Gamma(2m_1)} \tag{9a}$$

$$\times \sum_{l=1}^{i} \frac{(-1)^l \delta_{i-l}}{l!} (-i+l+l\,M)\Gamma(2(l+m_1)) \times \Gamma(l+m_1+m_2)\left(\frac{m_1}{m_2}\right)^{l}, i \geq 1. \tag{9b}$$

Meanwhile, $f_{\mathcal{D}_2}(y)$ is defined as

$$f_{\mathcal{D}_2}(y) = \sqrt{\frac{\Omega_2}{\Omega_1}} \left(\frac{1}{\Gamma(m_1)\Gamma(m_2)}\right)^{M} \sum_{k=0}^{M} \binom{M}{k} \left(2\left(\frac{m_2}{m_1}\right)^{m_2}\right)^{k} \times \sum_{i=0}^{\infty}\sum_{j=0}^{\infty} \frac{\lambda_{k,i}\Lambda_{k,j}\left(y\sqrt{\frac{\Omega_2}{\Omega_1}}\right)^{-2(i+k\,m_2)-j-1}}{\Gamma(-2(i+k\,m_2)-j)}, \tag{10}$$

where $\lambda_{k,i}$ is given by

$$\lambda_{k,0} = (\Gamma(m_1+m_2)\Gamma(-2m_2))^k \tag{11a}$$

$$\lambda_{k,i} = \frac{1}{i\,\Gamma(m_1+m_2)\Gamma(-2m_2)} \times \sum_{l=1}^{i} \frac{(-1)^l \lambda_{k,i-l}}{l!} (-i+l+l\,k)\Gamma(-2(l+m_2)) \times \Gamma(l+m_1+m_2)\left(\frac{m_2}{m_1}\right)^{l}, i \geq 1, \tag{11b}$$

provided $m_2 \notin \frac{1}{2}\mathbb{Z}^+$, and $\Lambda_{k,j}$ is given by

$$\Lambda_{k,0} = (\Gamma(m_1)\Gamma(m_2))^{M-k} \tag{12a}$$

$$\Lambda_{k,j} = \frac{1}{j\,\Gamma(m_1)\Gamma(m_2)} \sum_{l=1}^{j} \frac{(-1)^l \Lambda_{k,j-l}}{l!}(-j+l+l\,(M-k)) \times \Gamma\left(m_1+\frac{l}{2}\right)\Gamma\left(m_2-\frac{l}{2}\right)\left(\frac{m_2}{m_1}\right)^{\frac{l}{2}}, j \geq 1. \tag{12b}$$

Proof: The proof is given in the Appendix A. ∎

Corollary: The CDF of the sum in (3) can be expressed as a piece-wise function as

$$F_Y(y) = \begin{cases} F_{\mathcal{D}_1}(y), & 0 < y \leq \left(\frac{m_2}{m_1}\right)^{\frac{1}{2}} \\ F_{\mathcal{D}_1}\left(\sqrt{\frac{m_2}{m_1}}\right) + F_{\mathcal{D}_2}(y), & y > \left(\frac{m_2}{m_1}\right)^{\frac{1}{2}}, \end{cases} \tag{13}$$

where $F_{\mathcal{D}_1}(y)$ is defined as

$$F_{\mathcal{D}_1}(y) = \left(\frac{2\left(\frac{m_1}{m_2}\right)^{m_1}}{\Gamma(m_1)\Gamma(m_2)}\right)^M \sum_{i=0}^{\infty} \frac{\delta_i \left(y\sqrt{\frac{\Omega_2}{\Omega_1}}\right)^{2(i+m_1 M)}}{\Gamma(2\,(i+M\,m_1)+1)}, \tag{14}$$

where δ_i is given in (9). On the other hand, $F_{\mathcal{D}_2}(y)$ is given by

$$F_{\mathcal{D}_2}(y) = \left(\frac{1}{\Gamma(m_1)\Gamma(m_2)}\right)^M \sum_{k=0}^{M}\binom{M}{i}\left(2\left(\frac{m_2}{m_1}\right)^{m_2}\right)^k \times \sum_{i=0}^{\infty}\lambda_{k,i}\sum_{j=0}^{\infty}\Lambda_{k,j}\left(\frac{\Omega_2}{\Omega_1}\right)^{-(i+k\,m_2)-\frac{j}{2}} \times \frac{\left(y^{-2(i+k\,m_2)-j} - \left(\frac{m2}{m1}\right)^{-(i+k\,m_2)-\frac{j}{2}}\right)}{\Gamma(-2(i+k\,m_2)-j+1)}, \tag{15}$$

provided $m_2 \in \frac{1}{2}\mathbb{Z}^+$, where $\lambda_{k,i}$ and $\Lambda_{k,j}$ are given in (11) and (12), respectively.

Proof: The CDF of the sum in (3) can readily obtained by integrating (7) from zero to y, i.e., $(F_Y(y) = \int_0^y f_Y(u)du)$. This completes the proof. ∎

Given that the results obtained in (8) and (10) are expressed in terms of infinite series, truncation was necessary. Thus, we define the truncation errors for the PDF, as

$$\epsilon_f(y,\tau) \triangleq f_Y(y) - \tilde{f}_Y(y), \tag{16}$$

where $\tilde{f}_Y(y)$ represents the function truncated to the τ-th term. Therefore, for $0 < y \leq \left(\frac{m_2}{m_1}\right)^{\frac{1}{2}}$, we have

$$\epsilon_{f_{\mathcal{D}_1}}(y,\tau) = \sqrt{\frac{\Omega_2}{\Omega_1}}\left(\frac{2\left(\frac{m_1}{m_2}\right)^{m_1}}{\Gamma(m_1)\Gamma(m_2)}\right)^M \times \sum_{i=\tau}^{\infty}\frac{\delta_i\left(y\sqrt{\frac{\Omega_2}{\Omega_1}}\right)^{-1+2(i+Mm_1)}}{\Gamma(2(i+Mm_1))}, \tag{17}$$

and for $y > \left(\frac{m_2}{m_1}\right)^{\frac{1}{2}}$

$$\epsilon_{f_{\mathcal{D}_2}}(y,\tau) = \sqrt{\frac{\Omega_2}{\Omega_1}}\left(\frac{1}{\Gamma(m_1)\Gamma(m_2)}\right)^M \times \sum_{k=0}^{M}\binom{M}{k}\left(2\left(\frac{m_2}{m_1}\right)^{m_2}\right)^k \times \sum_{i=\tau}^{\infty}\sum_{j=\tau}^{\infty}\frac{\lambda_{k,i}\,\Lambda_{k,j}\left(y\sqrt{\frac{\Omega_2}{\Omega_1}}\right)^{-1-j-2(i+km_2)}}{\Gamma(-j-2(i+km_2))}. \tag{18}$$

In Section V, we illustrate how the truncation errors rapidly decrease as the number of terms in the series, τ, increases, showing truncation errors on the order of 10^{-10} for $\tau \geq 40$ and different parameter settings.

B. APPROXIMATE SUM STATISTICS

Let R be a RV following a Beta Prime distribution [41] with PDF and CDF given respectively by

$$f_R(r) = \frac{r^{-1+a}(1+r)^{-a-b}}{B(a,b)}, \tag{19}$$

$$F_R(r) = I_{\frac{r}{r+1}}(a,b), \tag{20}$$

where a, b are the shape parameters, $B(\cdot,\cdot)$ denotes the Beta function [42, eq. (6.2.1)] and $I_{(\cdot)}(\cdot,\cdot)$ symbolizes the incomplete Beta function [42, eq. (26.5.1)].

The raw moments of R have simple closed-form expressions, given by

$$\mathbb{E}[R^t] = \prod_{k=1}^{t}\frac{a+k-1}{b-k}, \tag{21}$$

where $t \in \mathbb{N}$ and $t < b$.

Using the moment matching approach, we derive an approximate expression for the sum of independent Fisher-Snedecor $\mathcal{F}$ variates based on the Beta Prime distribution. The choice of the Beta Prime distribution is due to the direct and close relationship with the Fisher-Snedecor $\mathcal{F}$ distribution. Moreover, as the Beta Prime distribution is a two-parameter PDF and its first two raw moments are given in a relatively simple and tractable form (i.e., without gamma or exponential functions), we only need to solve two

non-transcendental equations to find the appropriate Beta Prime PDF parameters, as will be shown shortly.

The parameters a and b of the Beta Prime distribution in (19) are determined by matching the first and second raw moments, i.e., $\mathbb{E}[R] = \mathbb{E}[Y]$ and $\mathbb{E}[R^2] = \mathbb{E}[Y^2]$.

Solving the resulting two equations for a and b, we obtain

$$a = \frac{\mathbb{E}[Y](\mathbb{E}[Y] + \mathbb{E}[Y^2])}{\mathbb{E}[Y^2] - \mathbb{E}[Y]^2} \tag{22}$$

$$b = 2 + \frac{\mathbb{E}[Y](\mathbb{E}[Y] + 1)}{\mathbb{E}[Y^2] - \mathbb{E}[Y]^2}. \tag{23}$$

The first moment of Y required in (22), can be obtained as

$$\begin{aligned}\mathbb{E}[Y] &= \mathbb{E}\left[\sqrt{\frac{\Omega_1}{\Omega_2}}\sum_{n=1}^{M} H_n\right] \\ &\overset{(a)}{=} M\sqrt{\frac{\Omega_1}{\Omega_2}}\mathbb{E}[H_n] \\ &\overset{(b)}{=} M\sqrt{\frac{m_2\Omega_1}{m_1\Omega_2}}\frac{\mathbb{E}\left[X_n'\right]}{\mathbb{E}\left[Z_n'\right]} \\ &= M\sqrt{\frac{m_2\Omega_1}{m_1\Omega_2}}\frac{\Gamma(\frac{1}{2}+m_1)\Gamma(-\frac{1}{2}+m_2)}{\Gamma(m_1)\Gamma(m_2)},\end{aligned} \tag{24}$$

where in step (a), we used the independence of H_n, and in step (b), we used the independence between X_n and Z_n.

Meanwhile, the second moment of Y required in (22) can be calculated as

$$\begin{aligned}\mathbb{E}[Y^2] &= \mathbb{E}\left[\left(\sqrt{\frac{\Omega_1}{\Omega_2}}\sum_{n=1}^{M} H_n\right)^2\right] \\ &= \frac{\Omega_1}{\Omega_2}\mathbb{E}\left[\left(\sum_{n=1}^{M}\frac{X_n'}{Z_n'}\right)^2\right] \\ &\overset{(a)}{=} \frac{\Omega_1}{\Omega_2}\left(\sum_{n=1}^{M}\mathbb{E}\left[\left(\frac{X_n'}{Z_n'}\right)^2\right] + 2\sum_{j=1}^{M}\sum_{i=1}^{j-1}\mathbb{E}\left[\frac{X_i'X_j'}{Z_i'Z_j'}\right]\right),\end{aligned} \tag{25}$$

where in step (a), we used the binomial expansion.

Finally, utilizing the independence between X_n and Z_n along with some algebraic simplifications, (25) reduces to

$$\begin{aligned}\mathbb{E}[Y^2] = \frac{\Omega_1}{\Omega_2}\Bigg(&\frac{m_2}{m_1}M(M-1)\left(\frac{\Gamma(\frac{1}{2}+m_1)\Gamma(m_2-\frac{1}{2})}{\Gamma(m_1)\Gamma(m_2)}\right)^2 \\ &+ M\frac{m_2}{m_1}\frac{\Gamma(1+m_1)\Gamma(-1+m_2)}{\Gamma(m_1)\Gamma(m_2)}\Bigg).\end{aligned} \tag{26}$$

Using (24) and (26) along with minor simplifications, a and b ultimately reduce to (27) and (28), as shown at the bottom of the next page, respectively, as displayed at the top the next page.

IV. PERFORMANCE ANALYSIS

In this section, we evaluate the performance of EGC receivers subject to Fisher-Snedecor $\mathcal{F}$ fading channels by deriving exact and approximate formulas for the OP and ABER.

A. SIGNAL-TO-NOISE RATIO

The instantaneous signal-to-noise ratio (SNR) of an M-branch EGC diversity receiver is given by [1]

$$\gamma = \frac{\rho}{M}\left(\sqrt{\frac{\Omega_1}{\Omega_2}}\sum_{n=1}^{M} H_n\right)^2 = \frac{\rho}{M}Y^2, \tag{29}$$

where $\rho = \frac{E_s}{N_0}$ is the average SNR per symbol, with E_s being the transmitted energy symbol and N_0 the power of the additive white Gaussian noise.

Using (7) in (29) and applying the variable transformation, we have that the PDF of the γ for the exact sum can be expressed as piecewise functions as

$$f_\gamma(\gamma) = \begin{cases} f_{\gamma_{\mathcal{D}_1}}(\gamma), & 0 < \gamma \leq \left(\frac{m_2\,\rho}{m_1\,M}\right) \\ f_{\gamma_{\mathcal{D}_2}}(\gamma), & \gamma > \left(\frac{m_2\,\rho}{m_1\,M}\right), \end{cases} \tag{30}$$

$$f_{\gamma_{\mathcal{D}_1}}(\gamma) = \frac{1}{2\gamma}\left(\frac{2\left(\frac{m_1\Omega_2\gamma M}{m_2\Omega_1\rho}\right)^{m_1}}{\Gamma(m_1)\Gamma(m_2)}\right)^M \sum_{i=0}^{\infty}\frac{\delta_i\left(\frac{\Omega_2\gamma M}{\Omega_1\rho}\right)^i}{\Gamma(2(i+M\,m_1))}, \tag{31}$$

$$\begin{aligned}f_{\gamma_{\mathcal{D}_2}}(\gamma) = \frac{1}{2}\sqrt{\frac{\Omega_2 M}{\Omega_1\gamma\rho}}&\left(\frac{1}{\Gamma(m_1)\Gamma(m_2)}\right)^M \sum_{k=0}^{M}\binom{M}{k}2^k\left(\frac{m_2}{m_1}\right)^{m_2 k} \\ &\times\sum_{i=0}^{\infty}\lambda_{k,i}\sum_{j=0}^{\infty}\frac{\Lambda_{k,j}\left(\sqrt{\frac{\Omega_2\gamma M}{\Omega_1\rho}}\right)^{-2(i+k\,m_2)-j-1}}{\Gamma(-2(i+k\,m_2)-j)}.\end{aligned} \tag{32}$$

From (30), the exact CDF of γ can be found as

$$F_\gamma(\gamma) = \begin{cases} F_{\gamma_{\mathcal{D}_1}}(\gamma), & 0 < \gamma \leq \left(\frac{m_2\,\rho}{m_1\,M}\right) \\ F_{\gamma_{\mathcal{D}_2}}(\gamma), & \gamma > \left(\frac{m_2\,\rho}{m_1\,M}\right), \end{cases} \tag{33}$$

where

$$\begin{aligned}F_{\gamma_{\mathcal{D}_1}}(\gamma) &= \int_0^{\gamma} f_{\gamma_{\mathcal{D}_1}}(u)\mathrm{d}u, \\ &= \left(\frac{2\left(\frac{\gamma M m_1\Omega_2}{m_2\rho\Omega_1}\right)^{m_1}}{\Gamma(m_1)\Gamma(m_2)}\right)^M \sum_{i=0}^{\infty}\frac{\delta_i\left(\frac{\gamma M\Omega_2}{\rho\Omega_1}\right)^i}{\Gamma(2i+2Mm_1+1)},\end{aligned} \tag{34}$$

and

$$\begin{aligned}F_{\gamma_{\mathcal{D}_2}}(\gamma) &= \int_{\left(\frac{m_2\,\rho}{m_1\,M}\right)}^{\gamma} f_{\gamma_{\mathcal{D}_2}}(u)\mathrm{d}u + F_{\gamma_{\mathcal{D}_1}}\left(\frac{m_2\,\rho}{m_1\,M}\right), \\ &= \left(\frac{1}{\Gamma(m_1)\Gamma(m_2)}\right)^M \sum_{k=0}^{M}\binom{M}{k}2^k\left(\frac{m_2}{m_1}\right)^{m_2 k} \\ &\quad\times\sum_{i=0}^{\infty}\lambda_{k,i}\sum_{j=0}^{\infty}\Lambda_{k,j}\left(\sqrt{\frac{\Omega_2}{\Omega_1}}\right)^{-2(i+k\,m_2)-j}\end{aligned}$$

$$\times \frac{\left(\left(\sqrt{\frac{\gamma M}{\rho}}\right)^{-2(i+k\,m_2)-j} - \left(\sqrt{\frac{m_2}{m_1}}\right)^{-2(i+k\,m_2)-j}\right)}{\Gamma(1-2(i+k\,m_2)-j)}. \tag{35}$$

Similar to the exact sum case, we utilize (19) in (29) to derive PDF of γ for the approximate sum, yielding

$$\widehat{f}_\gamma(\gamma) = \frac{\left(\frac{M}{\rho}\right)^{\frac{a}{2}} \gamma^{-1+\frac{a}{2}} (1+\sqrt{\frac{M\gamma}{\rho}})^{-a-b}}{2\,B(a,b)}. \tag{36}$$

From (36), the approximate CDF of γ can be obtained as

$$\begin{aligned}\widehat{F}_\gamma(\gamma) &= \int_0^\gamma \widehat{f}_\gamma(u)\mathrm{d}u \\ &= \frac{\gamma^{a/2}\Gamma(a)\left(\frac{M}{\rho}\right)^{a/2}\,{}_2\tilde{F}_1\left(a, a+b; a+1; -\sqrt{\frac{M\gamma}{\rho}}\right)}{B(a,b)},\end{aligned} \tag{37}$$

where ${}_2\tilde{F}_1(.,.;.;.)$ is the regularized hypergeometric function [43], a and b are given in (27) and (28), respectively.

B. OUTAGE PROBABILITY

The OP is a statistical measure that quantifies the probability that a communication system will not be able to achieve a certain performance. In other words, the OP is the probability that the received signal is below a pre-defined threshold, ζ, namely [44, eq. (43)]

$$P_{\text{out}} \triangleq \Pr[\gamma \le \zeta] = F_\gamma(\zeta). \tag{38}$$

From (33), the exact OP can be obtained as

$$P_{\text{out}} = F_\gamma(\zeta). \tag{39}$$

More interestingly, the asymptotic OP can be derived by taking the first of the sum in (34). This expression is of paramount importance in analyzing communications systems in high SNR. The asymptotic OP, in terms of code gain ($\mathcal{K}_{out}$) and diversity gain ($\mathcal{V}_{out}$), is given by

$$P_{out} \simeq (\mathcal{K}_{out}\,\rho)^{-\mathcal{V}_{out}}, \tag{40}$$

where $\mathcal{V}_{out} = M\,m_1$, and $\mathcal{K}_{out}$ is given by

$$\mathcal{K}_{out} = \frac{m_2\Omega_1}{M\zeta\,m_1\Omega_2}\left(\frac{B(m_1,m_2)\,\Gamma(2\,M\,m_1+1)^{\frac{1}{M}}}{2\Gamma(2\,m_1)}\right)^{\frac{1}{m_1}}. \tag{41}$$

Finally, from (37), the approximate OP can be computed as

$$\widehat{P}_{\text{out}} = \widehat{F}_\gamma(\zeta). \tag{42}$$

C. AVERAGE BIT ERROR RATE

The ABER represents the probability of an error occurring when receiving a bit transmitted over a communication channel. For our investigated scenario, the ABER is defined as [44, eq. (31)]

$$P_e \triangleq \int_0^\infty Q(\sqrt{2\,\xi\,\gamma}) f_\gamma(\gamma)\,d\gamma, \tag{43}$$

in which $Q(\cdot)$ is the Gaussian Q-function [4, eq. (4.1)] and ξ is a modulation parameter (e.g., $\xi = 1$ for binary phase shift keying (BPSK) modulation).

Now, considering the limits of integration due to the piece-wise function and with the aid of the complementary error function erfc(·) [42, eq. (7.1.2)], (43) can be re-written as

$$\begin{aligned}P_e = \frac{1}{2}\Bigg(&\int_0^{\frac{m_2\rho}{m_1 M}} \text{erfc}(\sqrt{\xi\,\gamma}) f_{\gamma_{\mathcal{D}_1}}(\gamma)\,d\gamma \\ &+ \int_{\frac{m_2\rho}{m_1 M}}^\infty \text{erfc}(\sqrt{\xi\,\gamma}) f_{\gamma_{\mathcal{D}_2}}(\gamma)\,d\gamma\Bigg).\end{aligned} \tag{44}$$

Substituting (31) and (32) in (44), the exact ABER can be computed as follows

$$P_e = P_{e_1} + P_{e_2} \tag{45}$$

where

$$\begin{aligned}P_{e_1} = &\left(\frac{2\left(\frac{m_1\Omega_2}{m_2\Omega_1}\right)^{m_1}}{\Gamma(m_1)\,\Gamma(m_2)}\right)^M \sum_{i=0}^\infty \frac{\delta_i\left(\frac{\Omega_2 M}{\Omega_1\,\xi\,\rho}\right)^{i+Mm_1}}{2\sqrt{\pi}\Gamma(2(i+Mm_1)+1)} \\ &\times\Bigg(\sqrt{\pi}\,\text{erfc}\left(\sqrt{\frac{m_2\xi\rho}{m_1 M}}\right)\left(\frac{m_2\xi\rho}{Mm_1}\right)^{i+Mm_1} \\ &-\Gamma\left(i+Mm_1+\frac{1}{2}, \frac{m_2\xi\rho}{Mm_1}\right)+\Gamma\left(i+Mm_1+\frac{1}{2}\right)\Bigg),\end{aligned} \tag{46}$$

and

$$P_{e_2} = \frac{1}{4}\sqrt{\frac{\Omega_2 M}{\Omega_1\rho}}\left(\frac{1}{\Gamma(m_1)\Gamma(m_2)}\right)^M \sum_{k=0}^M \binom{M}{k} 2^k \left(\frac{m_2}{m_1}\right)^{m_2 k}$$

$$a = M\sqrt{\frac{m_2\Omega_1}{m_1\Omega_2}}\frac{\frac{(M-1)\Gamma\left(m_1+\frac{1}{2}\right)\Gamma\left(m_2-\frac{1}{2}\right)}{\Gamma(m_1)\Gamma(m_2)} + \left(\sqrt{\frac{m_1\Omega_2}{m_2\Omega_1}} + \frac{\Gamma(m_1+1)\Gamma(m_2-1)}{\Gamma\left(m_1+\frac{1}{2}\right)\Gamma\left(m_2-\frac{1}{2}\right)}\right)}{\frac{\Gamma(m_1)\Gamma(m_1+1)\Gamma(m_2)\Gamma(m_2-1)}{\Gamma\left(m_1+\frac{1}{2}\right)^2\Gamma\left(m_2-\frac{1}{2}\right)^2} - 1} \tag{27}$$

$$b = \frac{1}{\frac{\Gamma(m_1+1)\Gamma(m_2-1)}{\Gamma\left(m_1+\frac{1}{2}\right)^2\Gamma\left(m_2-\frac{1}{2}\right)^2} - \frac{1}{\Gamma(m_1)\Gamma(m_2)}}\left[\frac{M-2}{\Gamma(m_1)\Gamma(m_2)} + \frac{\sqrt{m_1}\sqrt{\Omega_2}}{\sqrt{m_2}\sqrt{\Omega_1}\Gamma\left(m_1+\frac{1}{2}\right)\Gamma\left(m_2-\frac{1}{2}\right)} + \frac{2\Gamma(m_1+1)\Gamma(m_2-1)}{\Gamma\left(m_1+\frac{1}{2}\right)^2\Gamma\left(m_2-\frac{1}{2}\right)^2}\right]. \tag{28}$$

$$\times \sum_{i=0}^{\infty} \lambda_{k,i} \sum_{j=0}^{\infty} \frac{\Lambda_{k,j} \left(\frac{m_2\Omega_1}{m_1\Omega_2}\right)^{-i-\frac{j}{2}-km_2}}{-\sqrt{\frac{\pi M \Omega_2}{\rho \Omega_1}}\Gamma(1-2(i+k\,m_2)-j)} \times \left(\sqrt{\pi}\,\mathrm{erfc}\left(\sqrt{\frac{m_2\xi\rho}{m_1 M}}\right) - \sqrt{\frac{m_2\xi\rho}{m_1 M}} E_{i+\frac{j}{2}+km_2+\frac{1}{2}}\left(\frac{m_2\xi\rho}{Mm_1}\right)\right), \quad (47)$$

in which $\Gamma(\cdot\,,\,\cdot)$ represents the incomplete gamma function [42, eq. (6.5.3)] and $E_n(\cdot)$ is the exponential integral function [42, eq. (5.1.4)].

Similar to the OP analysis, but now by taking the first term of the series in (46) and by letting $\rho \to \infty$ in $\mathrm{erfc}\left(\sqrt{\frac{m_2\xi\rho}{m_1 M}}\right)$ and in $\Gamma\left(i+Mm_1+\frac{1}{2}, \frac{m_2\xi\rho}{Mm_1}\right)$, the asymptotic ABER in terms of code gain ($\mathcal{K}_e$) and diversity gain ($\mathcal{V}_e$)is given by

$$P_e \simeq (\mathcal{K}_e\,\rho)^{-\mathcal{V}_e}, \quad (48)$$

where $\mathcal{V}_e = M\,m_1$, and $\mathcal{K}_e$ is given by

$$\mathcal{K}_e = \frac{\xi\, m_1\, \Omega_2}{M\, m_2\, \Omega_1} \left(\frac{B\,(m_1, m_2) \left(\frac{2\sqrt{\pi}\Gamma(2Mm_1+1)}{\Gamma\left(Mm_1+\frac{1}{2}\right)}\right)^{\frac{1}{M}}}{2\Gamma\,(2m_1)} \right)^{\frac{1}{m_1}}. \quad (49)$$

The approximate ABER can be obtained by replacing (36) in (43), i.e.,

$$\widehat{P}_e = \frac{1}{2}\int_0^{\infty} \mathrm{erfc}(\sqrt{\xi\,\gamma})\widehat{f}_{\gamma}(\gamma)\,d\gamma. \quad (50)$$

Solving the integral in (50), the approximate ABER is given in closed form as

$$\widehat{P}_e = \frac{\left(\frac{M}{\rho}\right)^{\frac{1}{2}(-b-1)}}{2\sqrt{\pi}b(b+1)\Gamma(a+b)B(a,b)} \times \left(\frac{(-2b^2-2b)\left(\frac{M\xi^{\frac{1}{b}}}{\rho}\right)^{\frac{b}{2}} \mathcal{A}(a,b,\rho,M,\xi)}{\Gamma(a+1)^{-1}\Gamma(b-1)^{-1}} + b(a+b)\xi^{\frac{b+1}{2}}\Gamma\left(-\frac{b}{2}\right)\Gamma(a+b)\,\mathcal{B}(a,b,\rho,M,\xi) + (b+1)\sqrt{\frac{M}{\rho}}\left(\sqrt{\pi}b\Gamma(a)\Gamma(b)\left(\frac{M}{\rho}\right)^{b/2} - \xi^{b/2}\Gamma\left(\frac{1}{2}-\frac{b}{2}\right)\Gamma(a+b)\,\mathcal{C}(a,b,\rho,M,\xi)\right)\right) \quad (51)$$

where

$$\mathcal{A}(a,b,\rho,M,\xi) = {}_3F_3\left(\frac{1}{2}, \frac{a}{2}+\frac{1}{2}, \frac{a}{2}+1; \frac{3}{2}, 1-\frac{b}{2}, \frac{3}{2}-\frac{b}{2}; -\frac{\xi\rho}{M}\right) \quad (52)$$

$$\mathcal{B}(a,b,\rho,M,\xi) = {}_3F_3\left(\frac{b+1}{2}, \frac{a+b+1}{2}, \frac{a+b+2}{2}; \frac{3}{2}, \frac{b+2}{2}, \frac{b+3}{2}; -\frac{\xi\rho}{M}\right) \quad (53)$$

$$\mathcal{C}(a,b,\rho,M,\xi) = {}_3F_3\left(\frac{a+b}{2}, \frac{a+b+1}{2}, \frac{b}{2}; \frac{1}{2}, \frac{b+1}{2}, \frac{b+2}{2}; -\frac{\xi\rho}{M}\right) \quad (54)$$

in which ${}_pF_q(\cdot)$ is the the HypergeometricPFQ function given in [45]. In the upcoming section, the expressions in (46) and (47) were computed using numerical integration due to their high computational cost.

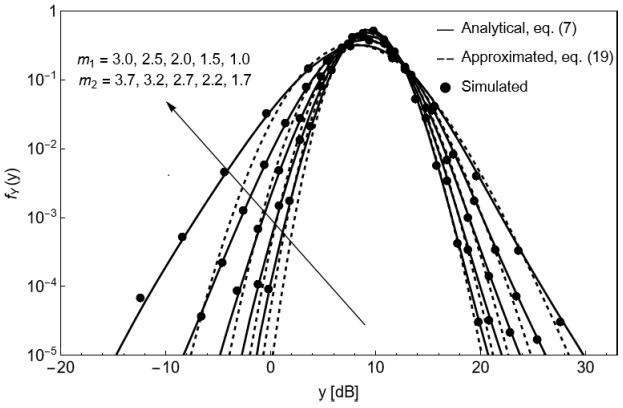

FIGURE 1. PDF of the analytical, approximated and simulated result with $M = 3$, $\Omega_1 = \Omega_2 = \{1.0, 1.0, 1.0, 1.0, 1.0\}$, $m_1 = \{1.0, 1.5, 2.0, 2.5, 3.0\}$ and $m_2 = \{1.7, 2.2, 2.7, 3.2, 3.7\}$.

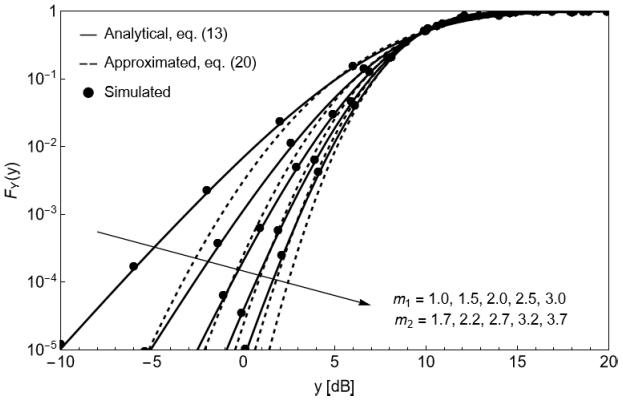

FIGURE 2. CDF of the analytical, approximated and simulated result with $M = 3$, $\Omega_1 = \Omega_2 = \{1.0, 1.0, 1.0, 1.0, 1.0\}$, $m_1 = \{1.0, 1.5, 2.0, 2.5, 3.0\}$ and $m_2 = \{1.7, 2.2, 2.7, 3.2, 3.7\}$.

V. RESULTS AND DISCUSSIONS

In this section, we validate our derived expressions through Monte Carlo simulations.[2] Additionally, we conduct a performance evaluation of EGC diversity receivers.

Figure 1 shows the analytical, approximate, and simulated PDFs of Y considering Ω_1 and Ω_2 equal to 1 and varying

[2]The number of realizations for Monte-Carlo simulations was set to 10^7.

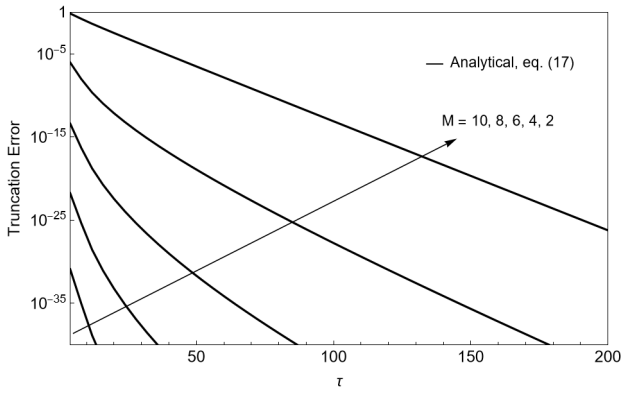

FIGURE 3. Truncation Error versus τ for $y = 1$ with $\Omega_1 = 1.0$, $\Omega_2 = 1.0$, $m_1 = 2.0$, $m_2 = 2.7$, and variation in M.

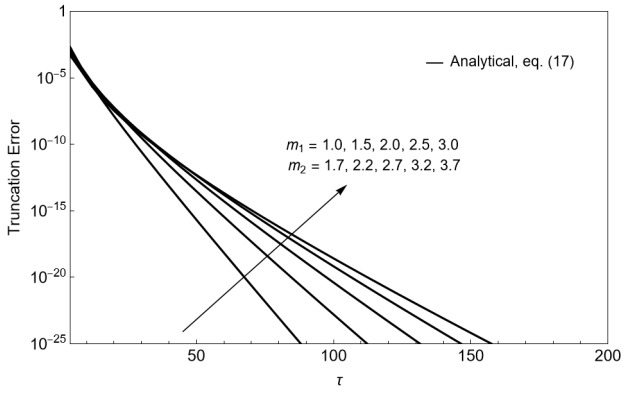

FIGURE 4. Truncation Error versus τ for $y = 1$ with $M = 3$, $\Omega_1 = \Omega_2 = \{1.0, 1.0, 1.0, 1.0, 1.0\}$, $m_1 = \{1.0, 1.5, 2.0, 2.5, 3.0\}$ and $m_2 = \{1.7, 2.2, 2.7, 3.2, 3.7\}$.

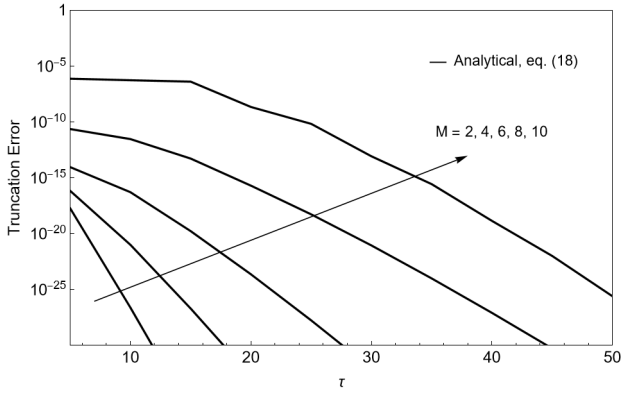

FIGURE 5. Truncation Error versus τ for $y = 25$ with $\Omega_1 = 1.0$, $\Omega_2 = 1.0$, $m_1 = 2.0$, $m_2 = 2.7$, and variation in M.

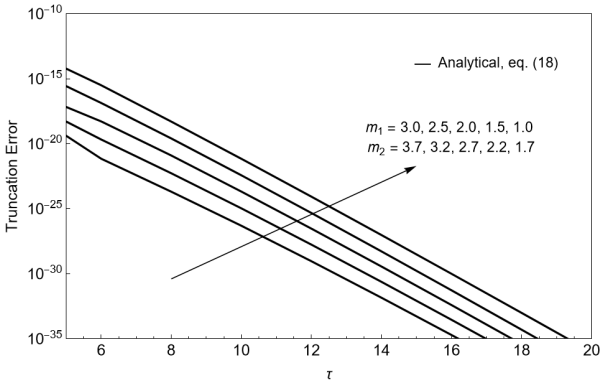

FIGURE 6. Truncation Error versus τ for $y = 25$ with $M = 3$, $\Omega_1 = \Omega_2 = \{1.0, 1.0, 1.0, 1.0, 1.0\}$, $m_1 = \{1.0, 1.5, 2.0, 2.5, 3.0\}$ and $m_2 = \{1.7, 2.2, 2.7, 3.2, 3.7\}$.

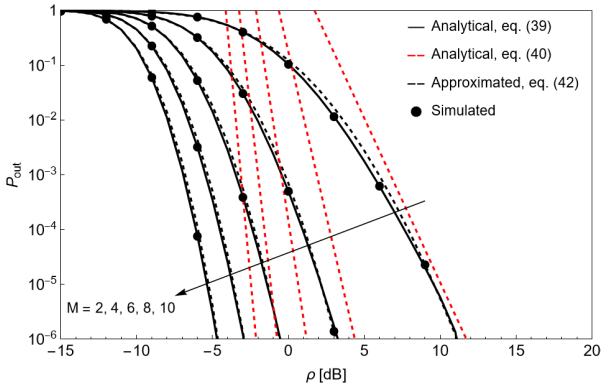

FIGURE 7. OP versus ρ for analytical, approximated and simulated result with $\Omega_1 = 1.0$, $\Omega_2 = 1.0$, $m_1 = 3.0$, $m_2 = 2.2$, and variation in M.

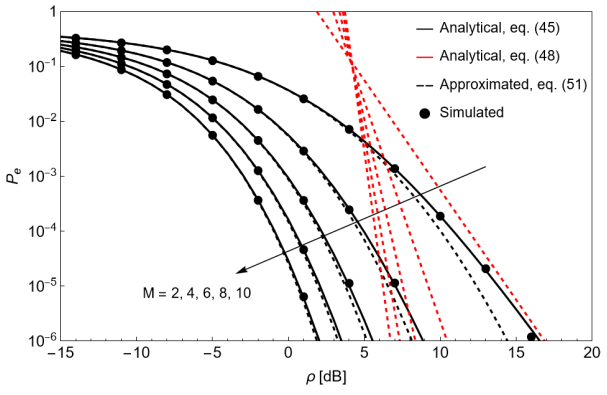

FIGURE 8. ABER versus ρ for analytical, approximated and simulated result with $\Omega_1 = 1.0$, $\Omega_2 = 1.0$, $m_1 = 2.0$, $m_2 = 2.7$, and variation in M.

values of m_1 and m_2. The analytical PDF curves show a perfect fit with the simulated data. On the other hand, regarding the approximate PDF, the figure shows that as m_1 and m_2 decrease the distance between the exact and the approximate values increase, i.e., the approximation does not fit the true values. More interestingly, it is possible to observe that the miss-matching between the approximate and true values is focused on the tails of the distribution. This result suggests that the Beta prime distribution follows the true distribution shape but has its limitations in approximating the tail distribution values. This occurs because higher-order moments are crucial for accurately characterizing tail distributions with the moment-matching method, and using only the first and second moments (for analytical convenience) can lead to minor inaccuracies at the extreme values of the distribution. Figure 2 illustrates the results of the CDF analysis of Y. Similar to the PDF analysis, the exact and simulated results show a total agreement while the approximation curves show a slight difference with respect to the exact curves as m_1 and m_2 decreases.

Analyzing Figs. 3–6, it can be noticed that for any parameter setting, the truncation errors for the PDF and the CDF decrease as the number of terms in their series, τ, grows. Moreover, from 3 and 4, it becomes apparent that the truncation error decreases as the value of M increases and the parameters m_1 and m_2 decrease. Similarly, upon examining Figs. 5 and 6, we can infer that the truncation error decreases as the value of M decreases and the parameters m_1 and m_2 increase.

Figure 7 displays the OP in terms of ρ for various values of M, the EGC diversity order. The figure indicates that for larger values of M, the system performance improves as expected. The analytical, approximate, and simulated results depicted show excellent consistency among them.

Figure 8 represents the ABER for various values of M, the EGC diversity order. As M increases, better ABER values are achieved. Using the approximation based on the Beta-Prime distribution (51), as the value of ρ increases, the results start to diverge; nevertheless, we still achieve good performance. Moreover, our asymptotic formulations (red curves in Figures 7 and 8) provide excellent fits as ρ increases.

VI. CONCLUSION

This paper aimed to assess the performance of EGC receivers over Fisher-Snedecor $\mathcal{F}$ fading channels. To do so, we derived exact and closed-form approximations for the sum statistics of the ratio of Nakagami-m RVs. All our derived formulations were thoroughly validated through numerical and Monte Carlo simulations.

The obtained sum statistics serve as valuable analytical tools for wireless engineers, as they can be applied in other wireless scenarios (e.g., multiple scattering communications, multihop relaying systems, and cascade fading channels), thereby enriching the overall body of knowledge.

APPENDIX A
PROOF EXACT SUM PDF

For motivation purposes, let us introduce the auxiliary RV:

$$H \triangleq \sum_{n=1}^{M} H_n. \tag{55}$$

The PDF of H_n has a closed-form expression and is given by [46, eq. (3.2)]

$$f_{H_n}(h_n) = \frac{2\,(m_1)^{m_1}\,(m_2)^{m_2}\,h_n^{-1+2m_1}}{B(m_1,m_2)}\left(m_2+m_1h_n^2\right)^{-m_1-m_2}. \tag{56}$$

After some algebraic manipulations, we can express (56) as

$$f_{H_n}(h_n) = \frac{2\left(\frac{m_1}{m_2}\right)^{m_1} h_n^{-1+2m_1}}{\Gamma(m_1)\Gamma(m_2)} \times G_{1,1}^{1,1}\left[\frac{m_1h_n^2}{m_2}\middle|\begin{matrix}1-m_1-m_2\\0\end{matrix}\right], \tag{57}$$

where $G_{a,c}^{d,b}[\cdot]$ is the Meijer G-function [47].

Now, with the aid of [48, eq. (07.34.02.0001.01)] along with some algebraic manipulations, we can rewrite (57) as

$$f_{H_n}(h_n) = \frac{2\left(\frac{m_1}{m_2}\right)^{m_1} h_n^{-1+2m_1}}{\Gamma(m_1)\Gamma(m_2)}\frac{1}{2\pi\mathbb{i}} \times \oint_{\mathcal{L}_s}\Gamma(m_1+m_2-s_1)\Gamma(s_1)\left(\frac{m_1h_n^2}{m_2}\right)^{-s_1} ds_1, \tag{58}$$

where $s_1 \in \mathbb{C}$ is a complex variable of integration, $\mathbb{i} = \sqrt{-1}$ is the imaginary unit, and $\mathcal{L}_s$ is a complex contour spanning counterclockwise all poles of $\Gamma(s_1)$.

Now, we proceed to compute the Laplace transform of the PDF of H_n, i.e.,

$$\mathcal{L}\{f_{H_n}\}(s) = \int_0^\infty \exp(-s\,h_n)\,f_{H_n}(h_n)\,dh_n, \tag{59}$$

in which $s \in \mathbb{C}$.

Substituting (58) into (59), interchanging the order of integration, and then evaluating the real inner integral with the assistance of [48, eq. (06.05.02.0001.01)], we obtain

$$\mathcal{L}\{f_{H_n}\}(s) = \frac{2\left(\frac{m_1}{m_2}\right)^{m_1} s^{-2m_1}}{\Gamma(m_1)\Gamma(m_2)}\frac{1}{2\pi\mathbb{i}}\oint_{\mathcal{L}_{s^\dagger}}\Gamma(m_1+m_2-s_1) \times \Gamma(s_1)\Gamma(2m_1-2s_1)s^{2s_1}\left(\frac{m_1}{m_2}\right)^{-s_1} ds_1, \tag{60}$$

where $\mathcal{L}_{s^\dagger}$ is a new complex contour that appears after solving the real inner integral. To avoid replicated poles, we choose $\mathcal{L}_{s^\dagger}$ to be a straight line parallel to the imaginary axis, starting at $-\infty\mathbb{i}+\varrho$ and ending at $+\infty\mathbb{i}+\varrho$ with $\varrho \in \mathbb{R}^+$ such that it separates the poles of $\Gamma(m_1+m_2-s_1)$ and $\Gamma(2m_1-2s_1)$ from those of $\Gamma(s_1)$.

Once $\mathcal{L}_{s^\dagger}$ is defined, we can now evaluate the complex integral in (60) via residues [49]. More specifically, as $\mathcal{L}_{s^\dagger}$ is a straight vertical line that splits the complex plane into two regions, one region containing the poles of $\Gamma(s_1)$, denoted as $\mathcal{D}_1$, and the other region containing the poles of $\Gamma(m_1+m_2-s_1)$ and $\Gamma(2m_1-2s_1)$, denoted as $\mathcal{D}_2$. Therefore, we must evaluate the complex integral in (60) by considering both regions. Certainly, the solution obtained after evaluating each region will possess its radius of convergence (ROC), as will be seen shortly.

1) $\mathcal{D}_1$ REGION

The poles contained in $\mathcal{D}_1$ are located at $s_1 = -i$ for $i = 0, 1, 2, \ldots$. Then, after applying the residue operation to (60) evaluated at these positions, we obtain the following solution:

$$\mathcal{L}\{f_{H_n,\mathcal{D}_1}\}(s) = \frac{2s^{-2m_1}\left(\frac{m_1}{m_2}\right)^{m_1}}{\Gamma(m_1)\Gamma(m_2)}\left(\sum_{i=0}^{\infty}\frac{1}{i!}\Gamma(i+m_1+m_2) \times \Gamma(2i+2m_1)\left(\frac{m_1}{m_2}\right)^{i}s^{-2i}\right). \tag{61}$$

The Laplace transform of the PDF of H, considering $\mathcal{D}_1$, is given by

$$\mathcal{L}\{f_{H,\mathcal{D}_1}\}(s) = \left(\mathcal{L}\{f_{H_n,\mathcal{D}_1}\}(s)\right)^M. \tag{62}$$

Replacing (61) into (62), we have

$$\mathcal{L}\{f_{H,\mathcal{D}_1}\}(s) = \left(\frac{2s^{-2m_1}\left(\frac{m_1}{m_2}\right)^{m_1}}{\Gamma(m_1)\Gamma(m_2)}\right)^M \left(\sum_{i=0}^{\infty}\frac{1}{i!}\Gamma(i+m_1+m_2) \times \Gamma(2i+2m_1)s^{-2i}\left(\frac{m_1}{m_2}\right)^i\right)^M. \tag{63}$$

Following non-trivial algebraic manipulations with the assistance of [39, eq. (0.314)], we get

$$\mathcal{L}\{f_{H,\mathcal{D}_1}\}(s) = \left(\frac{2s^{-2m_1}\left(\frac{m_1}{m_2}\right)^{m_1}}{\Gamma(m_1)\Gamma(m_2)}\right)^M \sum_{i=0}^{\infty}\delta_i\, s^{-2i}, \tag{64}$$

where δ_i is given in (9).

Now, we proceed to invert the (64) via

$$f_{H,\mathcal{D}_1}(h) = \left(\frac{1}{2\pi\mathrm{i}}\right)\oint_{\mathcal{L}_B}\exp(sh)\,\mathcal{L}\{f_{H,\mathcal{D}_1}\}(s)\,ds. \tag{65}$$

Plugging (64) into (65), and after a term-by-term inversion, we get

$$f_{H,\mathcal{D}_1}(h) = \left(\frac{2\left(\frac{m_1}{m_2}\right)^{m_1}}{\Gamma(m_1)\Gamma(m_2)}\right)^M \sum_{i=0}^{\infty}\frac{\delta_i\, h^{2(i+m_1M)-1}}{\Gamma(2(i+M\,m_1))}, \tag{66}$$

Using (66) and after a conventional transformation of variables (i.e., $Y = \sqrt{\Omega_1/\Omega_2}H$), the PDF of Y, considering $\mathcal{D}_1$, can be finally obtained as in (8), where its ROC lies within the strip $0 < y \leq \left(\frac{m_2}{m_1}\right)^{\frac{1}{2}}$.

2) $\mathcal{D}_2$ REGION

The poles contained in $\mathcal{D}_2$ are located at $s_1 = i+m_1+m_2$ and $s_1 = \frac{j}{2}+m_1$ for $i, j = 0, 1, 2, \ldots$. Accordingly, by applying the residue operation to (60) evaluated at these positions, we obtain the following solution:

$$\mathcal{L}\{f_{H_n,\mathcal{D}_2}\}(s) = \frac{1}{\Gamma(m_1)\Gamma(m_2)}\left(2\sum_{i=0}^{\infty}\frac{(-1)^i}{i!} \times \Gamma(i+m_1+m_2)\Gamma(-2i-2m_2)s^{2(i+m_2)}\left(\frac{m_1}{m_2}\right)^{-(i+m_2)} + \sum_{j=0}^{\infty}\frac{(-1)^j}{j!}\Gamma(m_2-\frac{j}{2})\Gamma(m_1+\frac{j}{2})s^j\left(\frac{m_1}{m_2}\right)^{-\frac{j}{2}}\right). \tag{67}$$

Recalling that H_n is formed by the ratio of i.i.d. RVs, then the Laplace transform of the PDF of H, considering $\mathcal{D}_2$, is given by

$$\mathcal{L}\{f_{H,\mathcal{D}_2}\}(s) = \left(\mathcal{L}\{f_{H_n,\mathcal{D}_2}\}(s)\right)^M. \tag{68}$$

Substituting (67) into (68), we get

$$\mathcal{L}\{f_{H,\mathcal{D}_2}\}(s) = \left(\frac{1}{\Gamma(m_1)\Gamma(m_2)}\right)^M\left(2\sum_{i=0}^{\infty}\frac{(-1)^i}{i!} \times \Gamma(i+m_1+m_2)\Gamma(-2i-2m_2)\left(\frac{m_1}{m_2}\right)^{-(i+m_2)}s^{2(i+m_2)} + \sum_{j=0}^{\infty}\frac{(-1)^j}{j!}\Gamma(m_2-\frac{j}{2})\Gamma(m_1+\frac{j}{2})s^j\left(\frac{m_1}{m_2}\right)^{-\frac{j}{2}}\right)^M. \tag{69}$$

Applying the binomial theorem in (69), we obtain

$$\mathcal{L}\{f_{H,\mathcal{D}_2}\}(s) = \left(\frac{1}{\Gamma(m_1)\Gamma(m_2)}\right)^M\sum_{k=0}^{M}\binom{M}{k} \times \left(2\sum_{i=0}^{\infty}\frac{(-1)^i}{i!}\Gamma(i+m_1+m_2) \times \Gamma(-2i-2m_2)\left(\frac{m_1}{m_2}\right)^{-(i+m_2)}s^{2(i+m_2)}\right)^k \times \left(\sum_{j=0}^{\infty}\frac{(-1)^j}{j!}\Gamma(m_2-\frac{j}{2})\Gamma(m_1+\frac{j}{2})\left(\frac{m_1}{m_2}\right)^{-\frac{j}{2}}s^j\right)^{M-k}. \tag{70}$$

After lengthy algebraic and series manipulations with the aid of [39, eq. (0.314)], we rewrite (70) as

$$\mathcal{L}\{f_{H,\mathcal{D}_2}\}(s) = \left(\frac{1}{\Gamma(m_1)\Gamma(m_2)}\right)^M\sum_{k=0}^{M}\binom{M}{k} \times \left(2\left(\frac{m_2}{m_1}\right)^{m_2}\right)^k s^{2m_2k}\sum_{i=0}^{\infty}\lambda_{k,i}\,s^{2i}\sum_{j=0}^{\infty}\Lambda_{k,j}\,s^j, \tag{71}$$

where $\lambda_{k,i}$ and $\Lambda_{k,i}$ are given in (11) and (12), respectively.

Now, we apply the inverse Laplace transform to (71), i.e.,

$$f_{H,\mathcal{D}_2}(h) = \left(\frac{1}{2\pi\mathrm{i}}\right)\oint_{\mathcal{L}_B}\exp(sh)\,\mathcal{L}\{f_{H,\mathcal{D}_2}\}(s)\,ds, \tag{72}$$

where $\mathcal{L}_B$ denotes the Bromwich contour.

Replacing (71) into (72), and after a term-by-term inversion, we obtain

$$f_{H,\mathcal{D}_2}(h) = \left(\frac{1}{\Gamma(m_1)\Gamma(m_2)}\right)^M\sum_{k=0}^{M}\binom{M}{k}\left(2\left(\frac{m_2}{m_1}\right)^{m_2}\right)^k \times \sum_{i=0}^{\infty}\lambda_{k,i}\sum_{j=0}^{\infty}\frac{\Lambda_{k,j}\,h^{-2(i+k\,m_2)-j-1}}{\Gamma(-2(i+k\,m_2)-j)}. \tag{73}$$

From (73) and after a straightforward transformation of variables (i.e., $Y = \sqrt{\Omega_1/\Omega_2}H$), the PDF of Y, considering $\mathcal{D}_2$, can be finally written as in (10), in which its ROC is given by the interval $y > \left(\frac{m_2}{m_1}\right)^{\frac{1}{2}}$.

REFERENCES

[1] L. S. Gordon, *Principles of Mobile Communication*. Berlin, Germany: Spinger, 2017.

[2] J. B. Andersen, T. S. Rappaport, and S. Yoshida, "Propagation measurements and models for wireless communications channels," *IEEE Commun. Mag.*, vol. 33, no. 1, pp. 42–49, Jan. 1995.

[3] D. da Costa, M. Yacoub, J. Filho, G. Fraidenraich, and J. Mendes, "Generalized Nakagami-*m* phase crossing rate," *IEEE Commun. Lett.*, vol. 10, no. 1, pp. 13–15, Jan. 2006.

[4] M. K. Simon and M.-S. Alouini, *Digital Communication Over Fading Channels*, 2nd ed., Hoboken, NJ, USA: Wiley, 2004.

[5] P. Ramírez-Espinosa and F. J. López-Martínez, "Composite fading models based on inverse gamma shadowing: Theory and validation," *IEEE Trans. Wireless Commun.*, vol. 20, no. 8, pp. 5034–5045, Aug. 2021.

[6] Z. Shengkui, Z. Qiuming, D. Xiuchao, L. Xinglin, C. Xiaomin, Q. Hongyan, and C. Bing, "Analysis and simulation for temporal correlated composite fading channels," in *Proc. 3rd Asia–Pacific Conf. Antennas Propag.*, Jul. 2014, pp. 690–693.

[7] C. Loo, "A statistical model for a land mobile satellite link," *IEEE Trans. Veh. Technol.*, vol. VT-34, no. 3, pp. 122–127, Aug. 1985.

[8] G. E. Corazza and F. Vatalaro, "A statistical model for land mobile satellite channels and its application to nongeostationary orbit systems," *IEEE Trans. Veh. Technol.*, vol. 43, no. 3, pp. 738–742, Aug. 1994.

[9] S. K. Yoo, S. L. Cotton, P. C. Sofotasios, M. Matthaiou, M. Valkama, and G. K. Karagiannidis, "The Fisher–Snedecor $\mathcal{F}$ distribution: A simple and accurate composite fading model," *IEEE Commun. Lett.*, vol. 21, no. 7, pp. 1661–1664, Jul. 2017.

[10] O. S. Badarneh, "Performance evaluation of wireless communication systems over composite α-μ/α-μ/gamma fading channels," *Wireless Pers. Commun.*, vol. 97, pp. 1235–1249, Nov. 2017.

[11] H. Al-Hmood and H. S. Al-Raweshidy, "Unified modeling of composite κ-μ/gamma, η-μ/gamma, and α-μ/gamma fading channels using a mixture gamma distribution with applications to energy detection," *IEEE Antennas Wireless Propag. Lett.*, vol. 16, pp. 104–108, 2017.

[12] F. Hansen and F. I. Meno, "Mobile fading—Rayleigh and lognormal superimposed," *IEEE Trans. Veh. Technol.*, vol. VT-26, no. 4, pp. 332–335, Nov. 1977.

[13] I. S. Ansari and M.-S. Alouini, "Asymptotic ergodic capacity analysis of composite lognormal shadowed channels," in *Proc. IEEE 81st Veh. Technol. Conf. (VTC Spring)*, May 2015, pp. 1–5.

[14] P. S. Bithas, "Weibull-gamma composite distribution: Alternative multipath/shadowing fading model," *Electron. Lett.*, vol. 45, no. 14, pp. 749–751, 2009.

[15] A. M. Mitic and M. M. Jakovljevic, "Second-order statistics in weibull-lognormal fading channels," in *Proc. 8th Int. Conf. Telecommun. Modern Satell., Cable Broadcast. Services*, Sep. 2007, pp. 529–532.

[16] R. Singh and M. Rawat, "Closed-form distribution and analysis of a combined Nakagami-lognormal shadowing and unshadowing fading channel," *J. Telecommun. Inf. Technol.*, vol. 4, no. 2016, pp. 81–87, Dec. 2016.

[17] V. M. Rodrigo-Peñarrocha, J. Reig, L. Rubio, H. Fernández, and S. Loredo, "Analysis of small-scale fading distributions in vehicle-to-vehicle communications," *Mobile Inf. Syst.*, vol. 2016, pp. 1–7, Jan. 2016.

[18] S. Atapattu, C. Tellambura, and H. Jiang, "Representation of composite fading and shadowing distributions by using mixtures of gamma distributions," in *Proc. IEEE Wireless Commun. Netw. Conf.*, Apr. 2010, pp. 1–5.

[19] A. J. Coulson, A. G. Williamson, and R. G. Vaughan, "A statistical basis for lognormal shadowing effects in multipath fading channels," *IEEE Trans. Commun.*, vol. 46, no. 4, pp. 494–502, Apr. 1998.

[20] A. Abdi and M. Kaveh, "K distribution: An appropriate substitute for Rayleigh-lognormal distribution in fading-shadowing wireless channels," *Electron. Lett.*, vol. 34, no. 9, p. 851, 1998.

[21] M. Nakagami, "The m-distribution—A general formula of intensity distribution of rapid fading," in *Statistical Methods in Radio Wave Propagation*. Amsterdam, The Netherlands: Elsevier, 1960, pp. 3–36.

[22] H. Suzuki, "A statistical model for urban radio propogation," *IEEE Trans. Commun.*, vol. COM-25, no. 7, pp. 673–680, Jul. 1977.

[23] F. A. García, H. C. Mora, and N. O. Garzón, "Improved exact evaluation of equal-gain diversity receivers in Rayleigh fading channels," *IEEE Access*, vol. 10, pp. 26974–26984, 2022.

[24] Q. T. Zhang, "Error rates for 4-branch equal-gain combining in independent Rayleigh fading: A simple explicit solution," *IEEE Commun. Lett.*, vol. 26, no. 2, pp. 269–272, Feb. 2022.

[25] Q. T. Zhang, "Simple and accurate polynomial formulas for error rates of high-order EGC in iid Rayleigh fading," *IEEE Wireless Commun. Lett.*, vol. 11, no. 7, pp. 1334–1338, Jul. 2022.

[26] F. D. A. García, H. R. C. Mora, and N. V. O. Garzón, "Novel expressions for Ricean sum distributions and densities," *IEEE Commun. Lett.*, vol. 25, no. 11, pp. 3513–3517, Nov. 2021.

[27] M. Ilic-Delibasic and M. Pejanovic-Djurisic, "MRC dual-diversity system over correlated and non-identical Ricean fading channels," *IEEE Commun. Lett.*, vol. 17, no. 12, pp. 2280–2283, Dec. 2013.

[28] N. O. Garzón, H. C. Mora, F. A. Garcl̀a, and C. D. Altamirano, "On the bit error probability and the spectral efficiency of opportunistic wireless transmissions in Rician fading channels," *IEEE Access*, vol. 9, pp. 49267–49280, 2021.

[29] F. D. A. García, F. R. A. Parente, G. Fraidenraich, and J. C. S. S. Filho, "Light exact expressions for the sum of Weibull random variables," *IEEE Wireless Commun. Lett.*, vol. 10, no. 11, pp. 2445–2449, Nov. 2021.

[30] F. D. A. García, F. R. A. Parente, M. D. Yacoub, and J. C. S. S. Filho, "Exact κ-μ sum statistics," *IEEE Wireless Commun. Lett.*, vol. 12, no. 7, pp. 1284–1288, Jul. 2023.

[31] M. Payami and A. Falahati, "Accurate variable-order approximations to the sum of α-μ variates with application to MIMO systems," *IEEE Trans. Wireless Commun.*, vol. 20, no. 3, pp. 1612–1623, Mar. 2021.

[32] C. Ben Issaid, M.-S. Alouini, and R. Tempone, "On the fast and precise evaluation of the outage probability of diversity receivers over α-μ, κ-μ, and η-μ fading channels," *IEEE Trans. Wireless Commun.*, vol. 17, no. 2, pp. 1255–1268, Feb. 2018.

[33] F. D. A. García, F. R. A. Parente, M. D. Yacoub, and J. C. S. S. Filho, "On the exact sum PDF and CDF of α-μ variates," *IEEE Trans. Wireless Commun.*, vol. 22, no. 8, pp. 5084–5095, Aug. 2023.

[34] O. S. Badarneh, D. B. Da Costa, P. C. Sofotasios, S. Muhaidat, and S. L. Cotton, "On the sum of Fisher–Snedecor $\mathcal{F}$ variates and its application to maximal-ratio combining," *IEEE Wireless Commun. Lett.*, vol. 7, no. 6, pp. 966–969, Dec. 2018.

[35] H. Du, J. Zhang, J. Cheng, and B. Ai, "Sum of Fisher–Snedecor $\mathcal{F}$ random variables and its applications," *IEEE Open J. Commun. Soc.*, vol. 1, pp. 342–356, 2020.

[36] F. S. Rizi and A. Falahati, "The generalized-Fisher composite fading model for the next generation of mobile communication systems," *Digit. Commun. Netw.*, Feb. 2023.

[37] K. Wang, T. Wang, Y. Chen, and M.-S. Alouini, "Sum of ratios of products for α-μ random variables in wireless multihop relaying and multiple scattering," in *Proc. IEEE 80th Veh. Technol. Conf. (VTC-Fall)*, Sep. 2014, pp. 1–5.

[38] O. S. Badarneh, P. C. Sofotasios, S. Muhaidat, S. L. Cotton, and D. B. Da Costa, "Product and ratio of product of Fisher–Snedecor $\mathcal{F}$ variates and their applications to performance evaluations of wireless communication systems," *IEEE Access*, vol. 8, pp. 215267–215286, 2020.

[39] I. S. Gradshteyn and I. M. Ryzhik, *Table of Integrals, Series, and Products*. Cambridge, MA, USA: Academic Press, 2014.

[40] D. Brennan, "Linear diversity combining techniques," *Proc. IRE*, vol. 47, no. 6, pp. 1075–1102, Jun. 1959.

[41] N. L. Johnson, S. Kotz, and N. Balakrishnan, *Continuous Univariate Distributions*, vol. 2. Hoboken, NJ, USA: Wiley, 1995.

[42] M. Abramowitz and I. A. Stegun, *Handbook of Mathematical Functions With Formulas, Graphs, and Mathematical Tables*, vol. 55, 10th ed., Washington, DC, USA: National Bureau of Standards, 1972.

[43] Wolfram Research. *Hypergeometric2F1Regularized*. Accessed: May 9, 2024. [Online]. Available: https://functions.wolfram.com/HypergeometricFunctions/Hypergeometric2F1Regularized/

[44] Y. Chen and C. Tellambura, "Distribution functions of selection combiner output in equally correlated Rayleigh, Rician, and Nakagami-*m* fading channels," *IEEE Trans. Commun.*, vol. 52, no. 11, pp. 1948–1956, 2004.

[45] Wolfram Research. *HypergeometricPFQ*. Accessed: May 16, 2024. [Online]. Available: https://functions.wolfram.com/HypergeometricFunctions/HypergeometricPFQ/

[46] J. H. Curtiss, "On the distribution of the quotient of two chance variables," *Ann. Math. Statist.*, vol. 12, no. 4, pp. 409–421, Dec. 1941.

[47] Wolfram Research. *MeijerG*. Accessed: Dec. 2, 2023. [Online]. Available: https://reference.wolfram.com/language/ref/MeijerG.html

[48] Wolfram Research. *Wolfram Research*. Accessed: Dec. 12, 2023. [Online]. Available: http://functions.wolfram.com

[49] E. Kreyszig, *Advanced Engineering Mathematics*, 10th ed., Hoboken, NJ, USA: Wiley, 2010.

SÁVIO VIEIRA LACERDA DA SILVA received the bachelor's degree in electrical engineering from the Federal University of Ouro Preto (UFOP), where he had the opportunity to spend a semester on international academic mobility in the Integrated master's program in electrical and computer engineering with the University of Porto, Portugal, funded by the Santander Ibero-American Scholarships Program. He is currently pursuing the master's degree in postgraduate program with the Faculty of Electrical and Computer Engineering (FEEC), State University of Campinas (UNICAMP), specializing in telecommunications and telematics. During his undergraduate studies, he gained practical experience through two significant internships. The first was in industrial maintenance at Arcelor Mittal Monlevade, providing valuable insights into the practical application of theoretical knowledge in industrial settings. The second internship was in the field of telecommunications at the headquarters of the Agência Nacional de Telecomunicações (Anatel), Brasília, contributing to his understanding of the regulatory sector. At UFOP, he also distinguished himself through research involvement, participating in scientific initiation in the field of signal processing, and contributing to three extension projects.

LENIN PATRICIO JIMÉNEZ was born in Loja, Ecuador, in 1995. He received the B.Sc. degree in electronics and telecommunications engineering from Universidad Técnica Particular de Loja (UTPL), Loja, in 2018; and the M.Sc. degree in electrical engineering from the School of Electrical and Computer Engineering (FEEC), State University of Campinas (UNICAMP), São Paulo, Brazil, in 2022. Currently, he is pursuing the Ph.D. degree with FEEC, UNICAMP. Since 2020, he has been worked together with the ELDORADO Research Institute in multiple projects related to AI. Since 2020, he has been part of the Wireless Technology Laboratory (WissTek), FEEC-UNICAMP. His research interests include wireless communications, MIMO systems, radar systems, and machine learning.

FERNANDO DARÍO ALMEIDA GARCÍA (Senior Member, IEEE) received the B.Sc. degree in electronics and telecommunications engineering from Armed Forces University–ESPE, Quito, Ecuador, in 2012, and the M.Sc. and Ph.D. degrees in electrical engineering from the School of Electrical and Computer Engineering (FEEC), State University of Campinas (UNICAMP), São Paulo, Brazil, in 2015 and 2021, respectively.

From 2014 to 2020, he worked together with Bradar Indústria S. A. and Embraer Defense and Security, in the development of innovative radar signal processing techniques. From 2021 to 2023, he was a Postdoctoral Researcher with the Wireless Technology Laboratory (WissTek), FEEC-UNICAMP. Since 2023, he has been a Postdoctoral Fellow with the Harvard John A. Paulson School of Engineering and Applied Sciences, Harvard University, Cambridge, MA, USA. His research interests include statistical signal processing, wireless communications, radar systems, complex analysis, and channel modeling.

SANTOSH KUMAR received the Ph.D. degree in physics from Jawaharlal Nehru University, India, in 2011. He was a Postdoctoral Researcher with AG Guhr, University of Duisburg-Essen, Germany, in 2013. Currently, he is an Associate Professor with the Department of Physics, Shiv Nadar University, India. His research interests include random matrix theory, supersymmetry, and their applications to varied fields of knowledge. His research interests include multivariate statistics, information and communication theory, and quantum transport problem.

JOSÉ CÂNDIDO SILVEIRA SANTOS FILHO (Member, IEEE) received the B.Sc. (Hons.), M.Sc., and Ph.D. degrees in electrical engineering from the School of Electrical and Computer Engineering (FEEC), State University of Campinas (UNICAMP), Campinas, São Paulo, Brazil, in 2001, 2003, and 2006, respectively. From 2006 to 2009, he was a Postdoctoral Fellow with the Wireless Technology Laboratory (WissTek), FEEC-UNICAMP, where he is currently an Associate Professor. Since 2011, he has been regularly consulted for Bradar Indútria S.A., a branch of Embraer Defense and Security, to assist in the development of advanced radar techniques and systems. From June 2018 to September 2019, he was a Visiting Researcher with Harvard University. He has published more than 100 technical articles, about half of which are in international journals. His research interests include wireless communications and radar systems. His Ph.D. thesis was awarded an Honorary Mention by Brazilian Ministry of Education (CAPES) in the 2007 CAPES Thesis Contest. He has served as a reviewer for many prestigious journals and conferences worldwide.

EDUARDO RODRIGUES DE LIMA received the E.E. degree from the University of São Paulo State (UNESP) and the Ph.D. degree from the Technical University of Valencia-UPV, Spain. He is currently a Research and Development Manager with the Exploratory Hardware Design Department, Eldorado Research Institute and a Visiting Professor with UNICAMP, Campinas, Brazil. He has more than 20 years of experience in telecommunications systems. He coordinates several research and development projects related to microelectronics, embedded systems, smart grid, and the IoT. His current research interests include the implementation and theoretical aspects of physical layers of wireless and wired communications systems. He is an MCTI/CNPq Fellow of Technological Productivity.

GUSTAVO FRAIDENRAICH (Member, IEEE) was born in Pernambuco, Brazil, in 1977. He received the degree in electrical engineering from the Federal University of Pernambuco (UFPE), Brazil, and the M.Sc. and Ph.D. degrees from the State University of Campinas (UNICAMP), Brazil, in 2002 and 2006, respectively. From 2006 to 2008, he was a Postdoctoral Fellow with Stanford University (Star Laboratory Group), USA. Currently, he is an Assistant Professor with UNICAMP. He has published more than 50 international journal papers and over a hundred conference papers of the first line. His research interests include multiple antenna systems, cooperative systems, radar systems, and wireless communications in general. He was awarded the Young Researcher Scholarship of the Fundação de Amparo à Pesquisa do Estado de São Paulo (FAPESP), in 2009. He is president of the Technical Board at Venturus, a branch of Ericsson Company. He has been an Associate Editor of the ETT journal for many years.